# EXPERIMENT 1

## EDDY-COVARIANCE METHOD

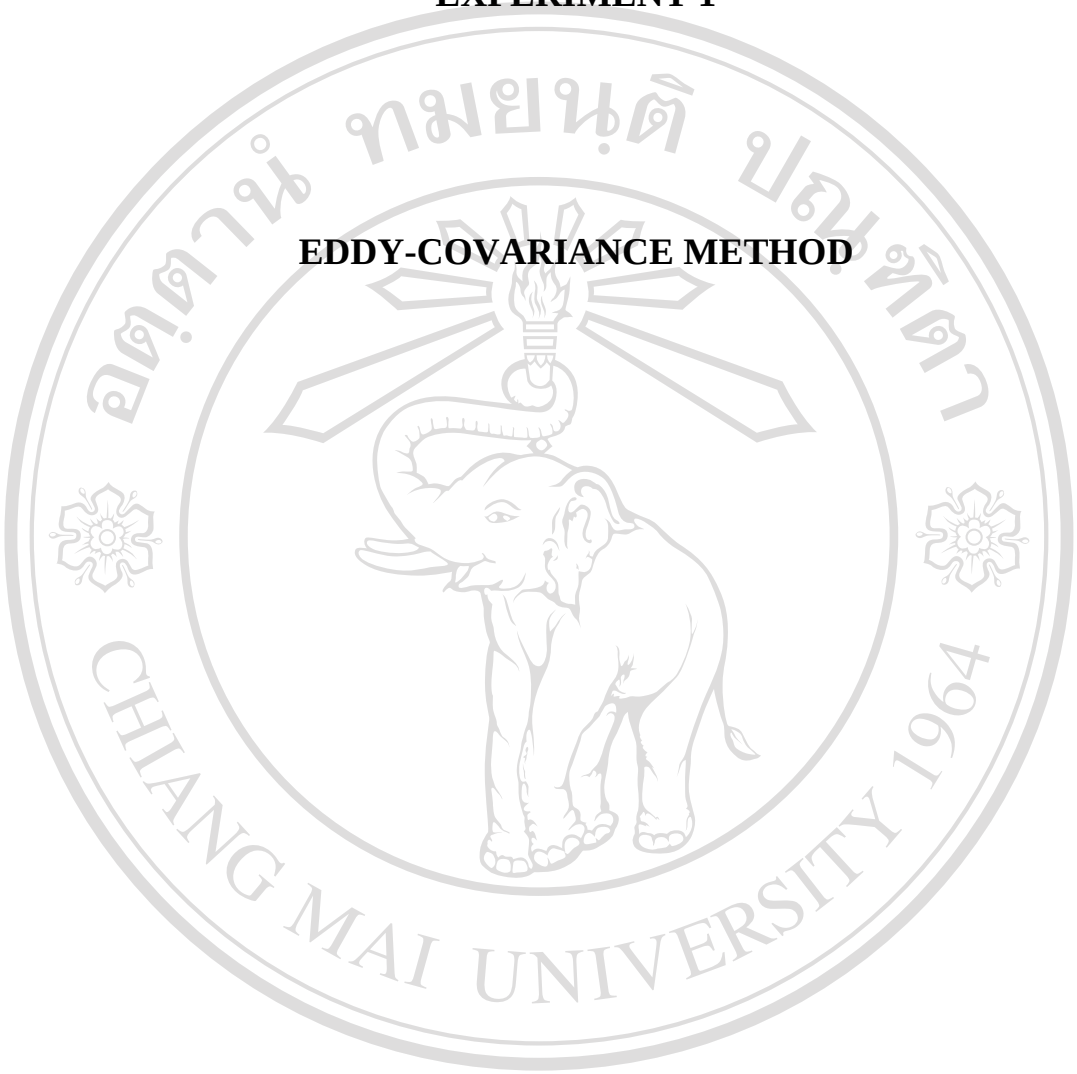

## Sub-experiment 1

# Influence of drought stress on the diurnal exchange of mass and energy between the atmosphere and a peanut canopy

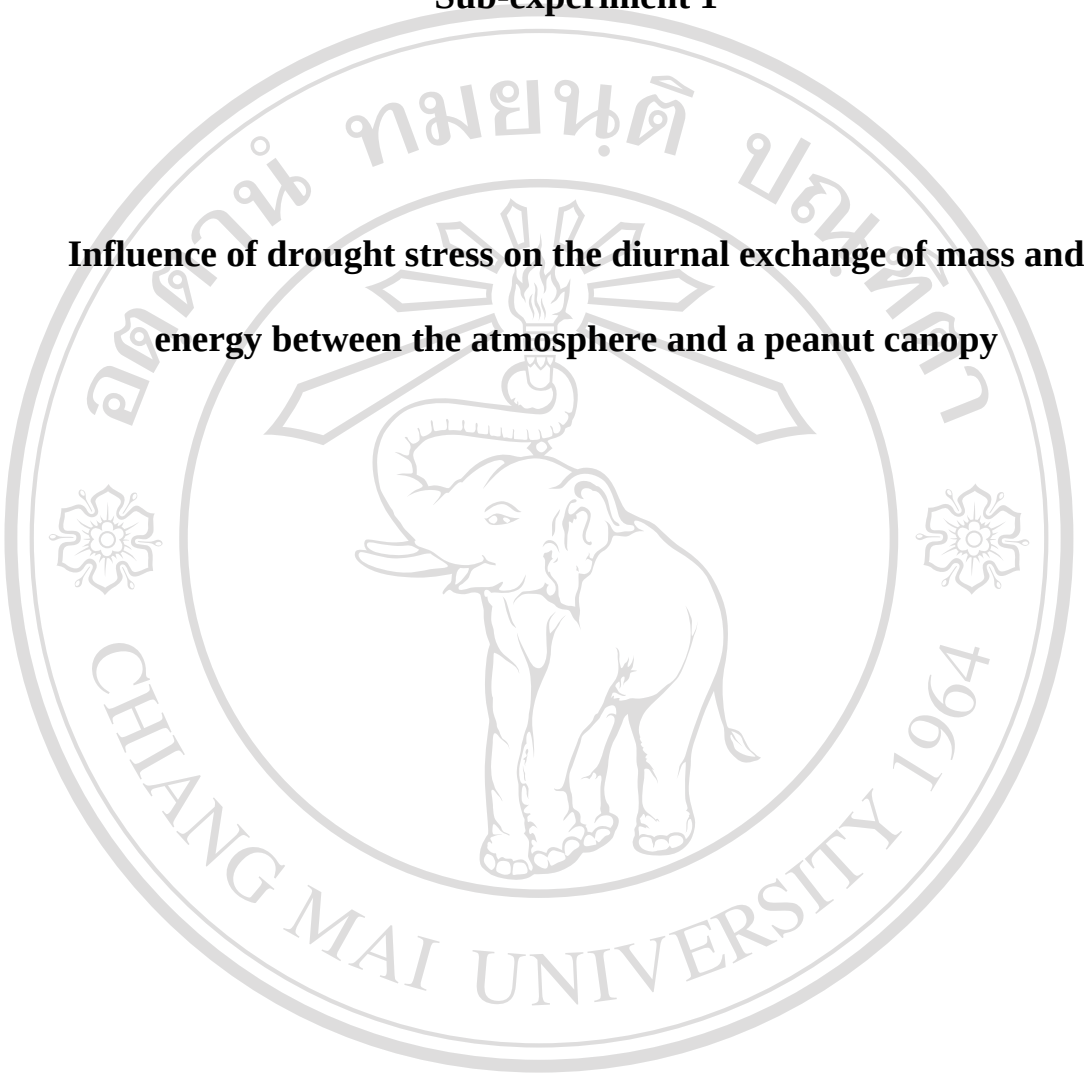

# INTRODUCTION

The development of regional and global climate models has increased the understanding of terrestrial carbon exchange at larger scales (Canadell *et al.*, 2000). There are now many studies through out the world assessing the environmental constraints on carbon and water vapor exchange of well-watered ecosystems including forests (e.g. Anthoni *et al.*, 2002; Carrara *et al.*, 2003; Hollinger *et al.*, 1999) and grasslands (e.g. Hammerle *et al.*, 2007; Wohlfahrt *et al.*, 2008; Xu and Baldocchi, 2004). A number of investigations have taken place on the fluxes of water and $CO_2$ from drought stress in forests (e.g. Granier *et al.*, 2007; Holst *et al.*, 2008; Law *et al.*, 2001; Vourlitis *et al.*, 2005) and grasslands (e.g. Aires *et al.*, 2008b; Fu *et al.*, 2006; Hao *et al.*, 2008; Hunt *et al.*, 2002; Li *et al.*, 2005; Nakano *et al.*, 2008; Wang *et al.*, 2008). As large networks of ecosystem studies have been organized (e.g. EUROFLUX, AMERIFLUX, ASAIFLUX), there has been increased recognition of a lack of information on the effects of soil water deficit and heat stress on non-forested ecosystems, especially agricultural ecosystems.

Agricultural ecosystems, the most active part in global carbon pool, are greatly affected by human activities (e.g. cultivation, irrigation, fertilization), which lead to large variation of *NEE*. Climate change affects carbon storage in these ecosystems since both photosynthetic uptake of carbon and loss of carbon through respiration of plant and soils are depend on temperature, moisture, and radiation (Aubinet *et al.*, 2009; Moureaux *et al.*, 2006; Saito *et al.*, 2005). The reasons for the net carbon uptake remain poorly understood, making reliable projections of how agroecosystems will

respond to the ongoing climate change. Therefore, it is important to increase the knowledge of the biogeophysical and biogeochemical processes in these ecosystems. Water availability is a limiting factor for plant growth in many part of the world and, over long time scales, the local water balance could play a significant role in determining the carbon uptake capacity of the terrestrial surface. An accumulation deficit in soil water can shift the positive absorption of carbon toward negative release into the atmosphere, which can then upset feedback relationships in the evaporative process. Drought also alters the seasonal development of leaf area and changes plant physiology, thus influencing both magnitude and time of maximal $CO_2$ fixation.

Peanut (*Arachis hypogaea* L.) is a major crop grown under both rainfed and irrigated conditions in the southeastern US. The state of Georgia produces the largest proportion of all peanuts and more than half of the production area is in rainfed condition (USDA, 2004). In this environment, peanut plants have to cope with unfavorable environmental factors such as drought stress. Drought affects nearly all aspects of plant growth and most physiological processes; however, the stress response depends on the intensity, rate, and duration of exposure and the stage of crop growth. Inconsistent effects of these environmental stresses on physiological depression have been reported in previous studies and extensively studied at the leaf level (Reddy *et al.*, 2003). Drought stress alters the development of leaf area and changes the plant physiology. As an accumulation deficit in soil water increases, plants reduce stomatal conductance as a mechanism to diminish water loss through transpiration. As a consequence, the $CO_2$ assimilation is also reduced. The decrease in conductance of mesophyll cell due to water deficit is attributed to the limitation of $CO_2$ assimilation and further to the reduction in photosynthesis. The long-term effect

of soil water deficit on canopy assimilation is a reduction in leaf area. Drought reduces leaf area by folding, wilting, slowing leaf expansion, and reducing the supply of carbohydrates (Collino *et al.*, 2001; Reddy *et al.*, 2003). The consequent reduction in leaf area determines a decrease in the crop's ability to capture light resources (Chapman *et al.*, 1993; Collino *et al.*, 2001), resulting in a negative influence on both crop productivity and dry matter production.

To our knowledge, the influence of drought stress on the underlying processes of *NEE* at ecosystem level over a peanut farm has not been investigated. In this study, the EC method was conducted in a rainfed peanut field during growing season. The main objectives were to (1) to examine the variation of daytime *NEE*, ecosystem evapotranspiration (*E*), surface conductance ($g_s$), ecosystem water use efficiency (*EWUE*), energy fluxes such as latent heat flux ($\lambda E$) and sensible heat flux (*H*), and relevant environmental factors over a rainfed peanut field in relation to drought stress; and (2) to illustrate the underlying physiological mechanism of depression of $CO_2$ and $H_2O$ fluxes.

# MATERIAL AND METHODS

## Site description

Figure 2.1 A photo of the experimental site in 2007 in a rainfed peanut field in Unadilla, Georgia, USA.



The experiment was conducted in a rainfed peanut field located in Unadilla, Georgia, USA (32° 10' 39.72" N, 83° 38' 24.48" W) in 2007 (Figure 2.1). The top 10 cm of soil is classified as sandy loam, composed of 74% of sand, 16% of silt, and 10% of clay with a bulk density of 1.19 g $cm^{-3}$, the field capacity was 0.118 $m^3$ $m^{-3}$ and the permanent wilting point was 0.042 $m^3$ $m^{-3}$. Total carbon and nitrogen content of soil were 0.43 and 0.03%, respectively. Soil was applied with 336 kg $ha^{-1}$ of

5:15:30 (N:P:K) fertilizer on DOY 93. Peanut (*Arachis hypogaea* L.) was planted with 6.6 kg $ha^{-1}$ of phorate on DOY 125. Herbicides included of Gramoxone (1.75 L $ha^{-1}$), Storm (1.17 L $ha^{-1}$), and 2, 4-DB (0.44 L $ha^{-1}$) were applied on DOY 157. Leaf spot and white mold were controlled using Bravo Ultrex (on DOY 197, DOY 232, and DOY 253) and Headline 2.09EC (on DOY 176 and DOY 211). Peanut was harvested on DOY 283 with the yield of 4783 kg $ha^{-1}$.

**Experimental measurements and data processing**

Fluxes of carbon dioxide, water vapor, heat and momentum were continuously measured using EC method (Figure 2.2) from DOY 172 to DOY 271. The flux system were mounted at 1.5 m above the ground, consisted of a three-dimensional sonic anemometer (CSAT3, Campbell Scientific, Logan, UT) and a fast response open-path $CO_2/H_2O$ infrared gas analyzer (Li 7500, Li-Cor Inc., Lincoln, NE). The three wind components, sonic virtual temperature, water vapor, and $CO_2$ density were sampled at rate of 10 *Hz*. Half-hourly fluxes were calculated on-line and collected by CR1000 dataloggers (Campbell Scientific, Logan, UT). All raw 10*Hz* data were saved to the compact flash card (Sandisk, Sunnyvale, CA) for later reprocessing. The eddy-covariance flux system was power by two 12 VDC deep cycle batteries that were charge by 120 W solar panels (Figure 2.2). The EC tower was located approximately at the centre of the field, at a point with a minimum fetch of 210 m in all directions.

Figure 2.2 Photo of the eddy-covariance tower consisting of the three-dimensional sonic anemometer and the fast response open-path $CO_2/H_2O$ infrared gas analyzer with the net radiometer on the top of tower. The system was power by two 12 VDC deep cycle batteries that were charge by 120 W solar panels.

The raw 10 *Hz* data from sonic anemometer (the fluctuations in three wind components and sonic temperature) and infrared gas analyzer (water vapor, $CO_2$ density, and pressure) were checked for spiking before calculating eddy-covariance fluxes, similar to the method described by (Vickers and Mahrt, 1997). The fluctuations in three wind components from sonic anemometer were also rotated according to planar fit rotation to align the sonic anemometer axis along the long-term streamlines (Wilczak *et al.*, 2001). Before half-hourly fluxes of $CO_2$ (*NEE*), latent heat ($\lambda E$: where $\lambda$ is the latent heat of evaporation and $E$ is the evapotranspiration),

and sensible heat (*H*) were calculated, the time series were linearly detrended. Finally, the flux data were then corrected for variations in air density due to fluctuation in water vapor and heat fluxes in accordance with Webb *et al.* (1980). The records collected during wet half hours and up to 1 h after rain events were rejected because of the poor performance of the open path gas analyzer in wet weather. The analyses were conducted using a C++ program written in-house.

It is recognized by the flux monitoring community that the EC method is likely to underestimate eddy fluxes under calm conditions at night, but there is no consensus as to how the best correct the problem. Most of the researchers screened the nighttime data on the basis of a friction velocity ($u_*$) threshold (Aubinet *et al.*, 2000; Goulden *et al.*, 1997; Papale *et al.*, 2006; Reichstein *et al.*, 2005). The determination of the $u_*$ threshold was applied using the online calculation in http://gaia.agraria.unitus.it/database/ eddyproc. The estimation of $u_*$ threshold values was followed the same principle as in Reichstein *et al.* (2005). Gaps in solar radiation, temperature, and precipitation data were filled with data from nearby meteorological station. Due to a high percentage (78.68%) of the rejected carbon flux data during calm night, nighttime flux data are not presented in this study.

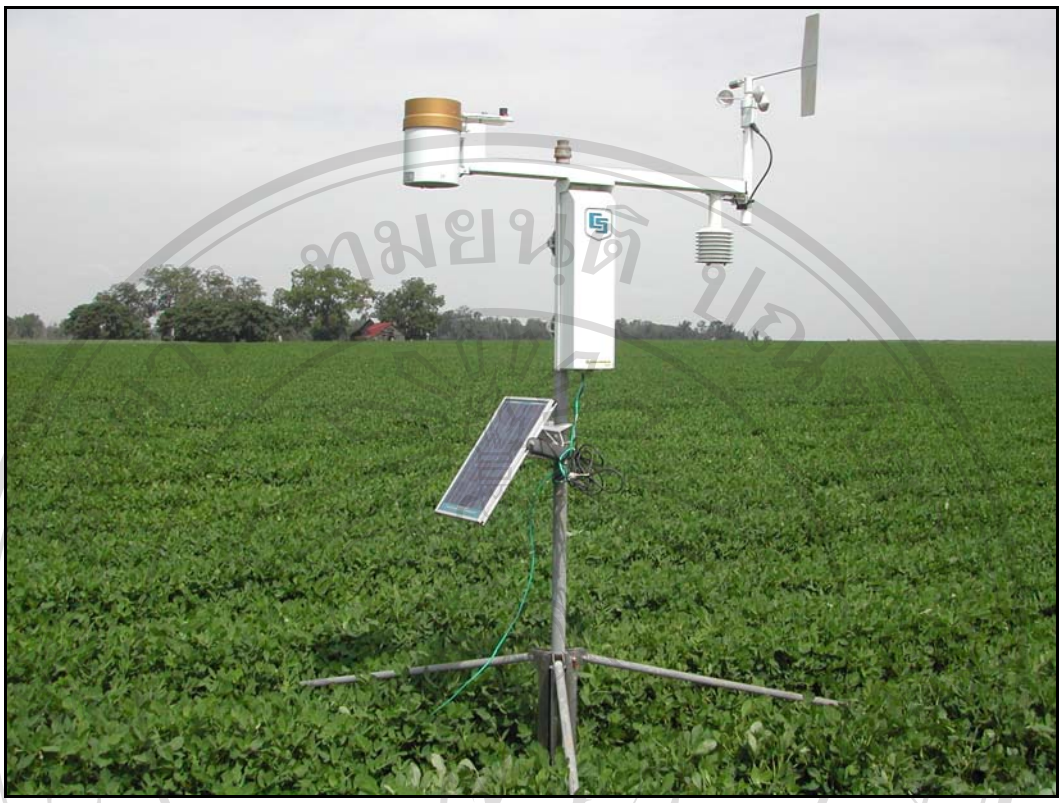

Figure 2.3 Photo of the ET106 (Campbell Scientific, Logan, UT) automatic weather station.

Along with the EC tower, standard meteorological and soil parameters were measured continuously with an array of sensors. Net radiation was measured using a net radiometer (Model NR-LITE, Kipp and Zonen USA Inc., Bohemia, New York) mounted at the EC tower, 1.8 m above the ground surface (Figure 2.2). Canopy temperature was measured at canopy height using a precision infrared thermocouple sensor at an accuracy of ± 0.4°C (IRTS-P5, Apogee Instrument Inc., Logan, UT). Belowground measurements was made at the base of tower, include soil temperature, and volumetric soil water content profiles. Soil temperature at depths of 0.02, 0.05, 0.08, and 0.30 m were measured with custom-built of the chromel-constantan thermocouple. Soil volumetric water content was measured with time domain

reflectometry sensor (CS615, Campbell. Scientific, Logan, UT) at depths of 0.02 and 0.02 to 0.05 m. All channels from meteorological and belowground measurements sensors were recorded 30-min average at dataloggers (CR10X, Campbell. Scientific, Logan, UT). The automatic weather station (ET106, Campbell Scientific, Logan, Utah) with 30-min average data output was installed at 2 m above the ground surface at the study site to measure air temperature, relative humidity, wind speed and wind direction, solar radiation, and precipitation. The station was powered by a 7 Ahr sealed-rechargeable battery that was charged with a 1000 W solar panel (Figure 2.3). In addition, the leaf area index (LAI) was determined at intervals of 7 to 10 days with an electronic leaf area meter (LAI-2000, Li-COR Inc., Lincoln, NE) throughout the season. The canopy temperature sensor was replaced on DOY 180.

**Data Analysis**

Ecosystem water use efficiency (*EWUE*) relates an ecosystem's exchange of carbon to its water use (i.e., evapotranspiration). In this study, *EWUE* was computed as (Laubach and Fritsch, 2002):

$$EWUE = -\frac{NEE}{E}, \quad (2.1)$$



The stomatal conductance or canopy conductance was used to assess stomatal control on $CO_2$ gas exchange and evapotranspiration. With no independent measurements of transpiration or soil evaporation available in this study, a clean separation of the two components is not possible with the eddy-covariance

measurements. Therefore, half-hourly surface conductance ($g_s$) was calculated by rearranging the Penman-Monteith equation (Monteith and Unsworth, 1990):

$$\frac{1}{g_s} = \left[\left(\frac{\Delta}{\gamma}\right)\beta - 1\right]\left(\frac{1}{g_a}\right) + \frac{\rho C_p VPD}{\gamma \lambda E}, \tag{2.2}$$

where $\Delta$ is the rate of change of saturation vapor pressure with temperature, $\gamma$ the pyschrometric constant, $\beta$ the Bowen ratio which is $H/\lambda E$, $\rho$ and $C_p$ the density and specific heat of air, respectively, *VPD* the vapor pressure deficit which is calculated from air temperature and relative humidity data, and $g_a$ the air conductance was obtained from sonic anemometer output as (Monteith and Unsworth, 1990):

$$\frac{1}{g_a} = \frac{u}{u_*^2} + 6.2u_*^{-0.67}, \tag{2.3}$$

where $u$ is the mean wind speed.

The coupling between the ecosystem surface and the atmospheric boundary layer can be determined by a dimensionless decoupling coefficient ($\Omega$), calculated on a half-hourly basis according to Jarvis and McNaughton (1986):

$$\Omega = \frac{(\Delta + \gamma)}{\Delta + \gamma(1 + g_a / g_s)}, \tag{2.4}$$

# RESULTS AND DISCUSSION

## Seasonal variation in environmental conditions and leaf area index

Figure 2.4 and 2.5 show the daily mean values of various climatic variables during the observation period from the late of June to September. The trends of daily averages of soil and canopy temperature across the growing season followed a pattern similar to that of air temperature ($T_a$). Daily average of soil, canopy and, air temperature varied from 21.7 to 31.7 °C, 20.6 to 33.7 °C, and 19.4 to 31.0 °C, respectively. Canopy temperature was slightly higher than soil temperature and air temperature, however, maximum values were observed in August (DOY 222) (Figure 2.4a). Total rainfall at the study site was 327 mm (Figure 2.4b). Soil water content (*SWC*) followed patterns of precipitation. Maximum daily average soil water content (0.135 $m^3$ $m^{-3}$) across the upper soil layer (0.02-0.05 m) occurred in early July (DOY 184). In particular, there were the large events of a gradual decrease in soil water content below wilting point (0.042 $m^3$ $m^{-3}$) on DOY 217-228 and DOY 250-255, suggesting that peanut plants may have experienced water stress during those periods (Figure 2.4b).

The daily total solar radiation was high in the early peanut growing season and gradual decrease through out the end of growing season (Figure 2.5a). The trends of daily average of vapor pressure deficit (*VPD*) across the growing season showed a pattern similar to air temperature which the maximum values (17.8 hPa and 31.0 °C for *VPD* and $T_a$, respectively) were observed on the same day (Figure 2.4a and 2.5b). LAI rapidly increased during crop development reaching the maximum value of 7.81

$m^2$ $m^{-2}$ in early August. While the minimum LAI of 2.92 $m^2$ $m^{-2}$ was found during water shortage (DOY 217-228).

The LAI reduction is due to either by drought-induced limitation of leaf area expansion or by temporary leaf wilting or rolling during periods of severe stress (Chapman *et al.*, 1993; Clifford *et al.*, 1993). With 52 mm of total precipitation on DOY 235, LAI showed an evident recovery reaching the values of 5.06 $m^2$ $m^{-2}$ and then steadily declined through out the end of study period as the plant senesced (Figure 2.5).

The interested data presented in this paper were obtained on the clear days over three periods: DOY 210 to 216, DOY 220 to 227, and DOY 248 to 254. During DOY 210 to 216, according to the Boote (1982) classification scheme for peanut development, the canopy was at stage R6 (pod-filling period) with 0.078 ± 0.027 $m^3$ $m^{-3}$ of daily average soil water content. Therefore, during DOY 210 to 216 was represented to the reproductive growth period with non-stress. The average daytime air temperature and daytime canopy temperature during this period were 28.3 ± 3.0 and 33.4 ± 5.9 °C, respectively. Both air and canopy temperature increased over the daytime reaching the maximum in the late afternoon (16:30 h to 17:00 h) (Figure 2.7a). Diurnal trends in vapor pressure deficit (*VPD*) followed those in air temperature and canopy temperature with reached the maximum at 20.5 ± 3.9 hPa at 16:30 h (Figure 2.7a). During DOY 220 to 227, the canopy was at stage R6 (pod-filling period) with 0.037 ± 0.002 $m^3$ $m^{-3}$ of daily average soil water content, which represented to the reproductive growth period with water stress. During this period, air temperature, canopy temperature, and *VPD* were higher than those measured during DOY 210 to 216(Figure 2.8a). The average daytime air temperature and

daytime canopy temperature during this period were 32.7 ± 4.1 and 36.4 ± 6.0 °C, respectively. *VPD* rapidly increased over the daytime reaching the maximum at 39.3 ± 8.3 hPa in the late afternoon (16:30 h) (Figure 2.8a). During DOY 248 to 254, the canopy was at stage R7 (early maturity period) with 0.035 ± 0.009 $m^3$ $m^{-3}$ of daily average soil water content, which represented to the maturity growth period with water stress. During this period, air temperature, canopy temperature, and *VPD* were lower than those observed during DOY 222 to 227 (Figure 2.9a). The average daytime air temperature and daytime canopy temperature during this period were 28.3 ± 2.6 and 30.0 ± 5.9 °C, respectively. *VPD* increased over the daytime reaching the maximum at 22.8 ± 3.4 hPa in the afternoon (15:00 h) (Figure 2.9a).

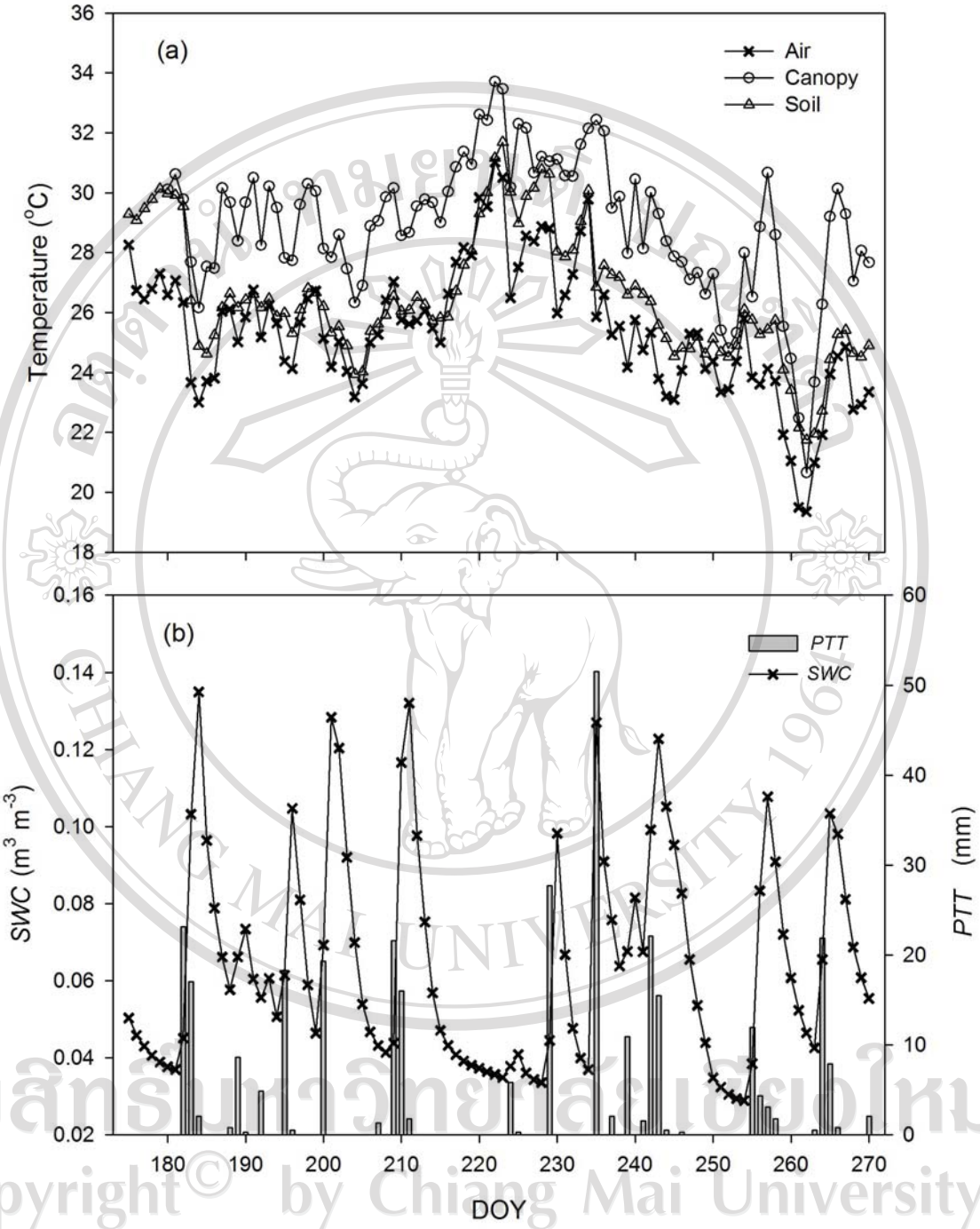


Figure 2.4 Daily averages of (a) air temperature, canopy temperature, and soil temperature at the depth of 2 cm, (b) soil water content (*SWC*) at the depth of 2-5 cm and the daily total precipitation (*PPT)* over the course of the study. DOY means days of year.

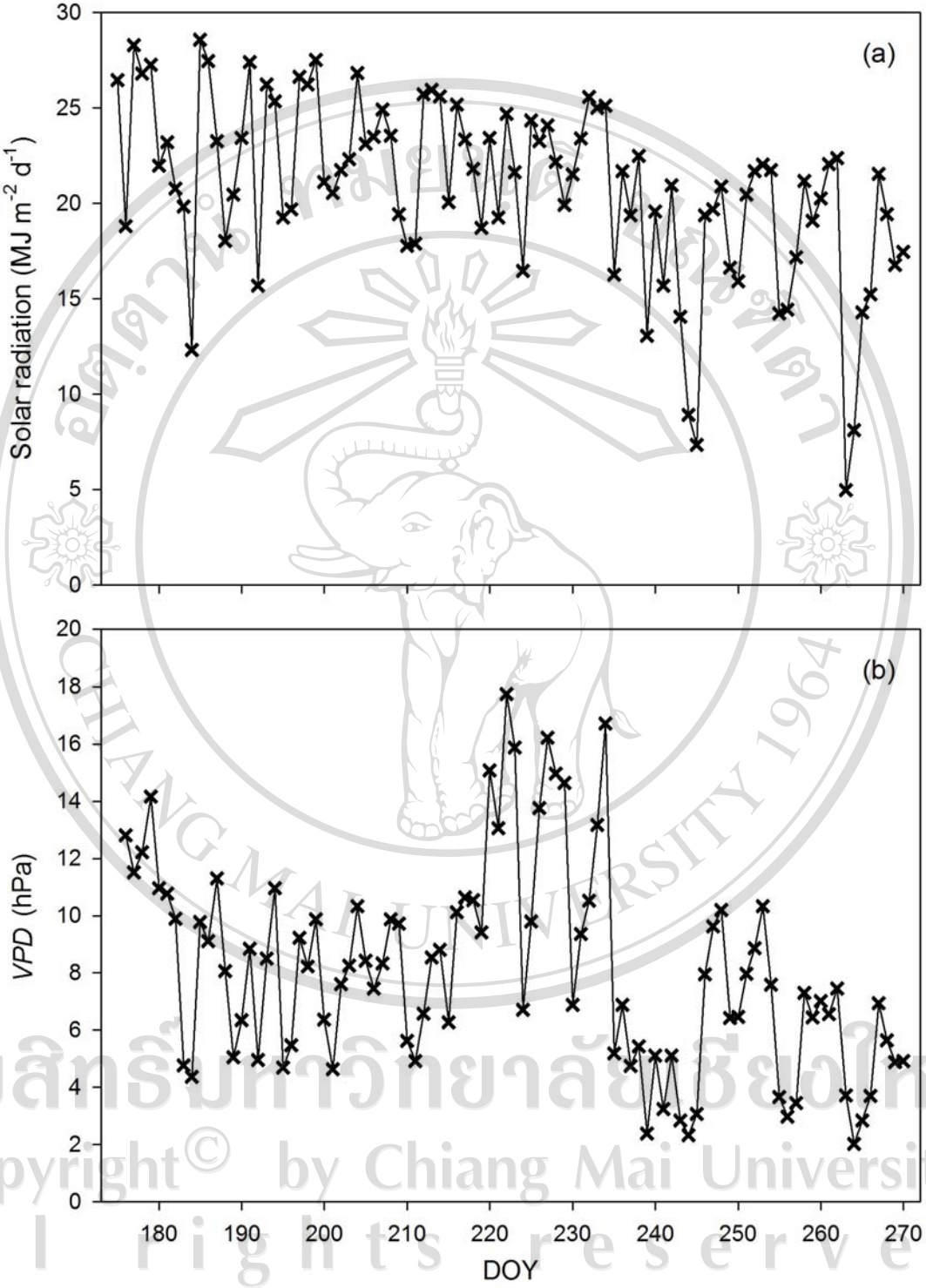




Figure 2.5 Daily total (a) solar radiation and (b) daily average of vapor pressure deficit (*VPD*) over the course of the study. DOY means days of year.

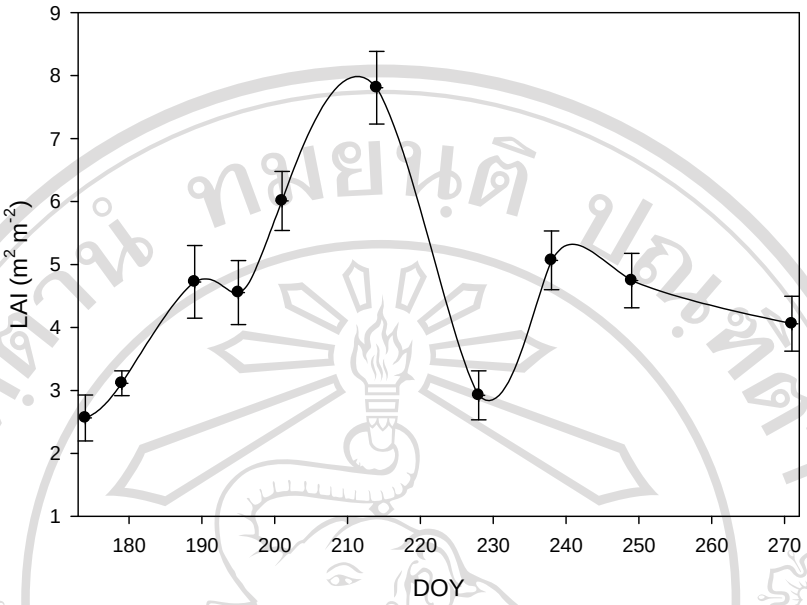


Figure 2.6 The trends in leaf area index (LAI) ± standard deviation over the course of the study.

**Diurnal patterns of the partitioning of available energy**

It is commonly thought that the partitioning pattern of the available energy is principally governed by environmental factors such as solar radiation, soil and air temperatures, wind regime, soil water availability, ecophysiological feather of plants, and canopy architecture (LAI, species composition, phenology, etc.) (e.g. Baldocchi, 1994a; Baldocchi, 1994b; Baldocchi, 1997). During the growing season, the partitioning of *Rn* into *H* and *λE* rather differently at different growth stages of canopy and available soil water. During the reproductive growth period with non-stress (DOY 210 to 216), half-hourly peak values of *Rn* ranged from 550 to 650 W $m^{-2}$ (Figure 2.7b). The daytime *λE* was strongly couple with *Rn* (Figure 2.7b). The percentage of *Rn* consumed by *LE* was fairly high. Midday values (12:00 h to 16:00 h, the same

hereafter) of $\lambda E/Rn$ were more than 60%, which is reasonable because the peanut plant was not water-limited. The sensible heat flux was a very minor part in $Rn$, the midday mean value of $H$ proportion was about 4%. Bowen ratio ($\beta$) in this period increased in the early morning and reached the peak of 0.30 at around 9:30 h. Midday $\beta$ was 0.06 in this period.

During the reproductive growth period with water stress (DOY 222 to 227), half-hourly peak values of $Rn$ were generally between 520 to 590 W $m^{-2}$ (Figure 2.8b). The daytime $\lambda E$ still dominated $Rn$ during this period. However, at midday $H$ become the main consumer of $Rn$. Midday values of $\lambda E/Rn$ were generally less than 50%. Midday Bowen ratio in this period increased to larger than unity, suggesting that the energy partitioning was $H$-dominated.

During the maturity growth period with water stress (DOY 248 to 254), half-hourly peak values of $Rn$ varied between 500 to 590 W $m^{-2}$ (Figure 2.9b). The daytime $\lambda E$ was the dominant consumption resource $Rn$ and followed similar to the pattern for $Rn$. Unlike $\lambda E$, $H$ had no significant diurnal variation (Figure 2.9b). Midday values of $\lambda E/Rn$ were about 60%. Similar to the period of DOY 210 to 216, $\beta$ in this period increased in the early morning and reached the peak of 0.33 at around 9:30 h. However, the midday $\beta$ in this period (0.18) was higher than that period of DOY 210 to 216 (0.06).



Kar and Kumar (2007) used a Bowen ratio micrometeorological method to measure the surface energy fluxes over irrigated peanut during winter (dry) season in eastern India. They found that $\beta$ was higher during early (before branching) and senescence (after seed filling) stages of peanut growth which was due to higher $H$ and lower $\lambda E$ during those periods. Moreover, Kar and Kumar (2007) also investigated a

sharp fall of $\beta$ during the peak growth stage when LAI was maximum. Similarly, the present study reveled that $\beta$ was small during the peak peanut growth stage with non environmental stress (DOY 210 to 216) which was due to higher LAI led to grater transpiration and therefore $\lambda E$ was higher during that period. There was a sharp increase of $\beta$ during the peak peanut growth stage when peanut subject to water stress (DOY 222 to 227) which was due to stomata closer led to lower $\lambda E$ during this period.

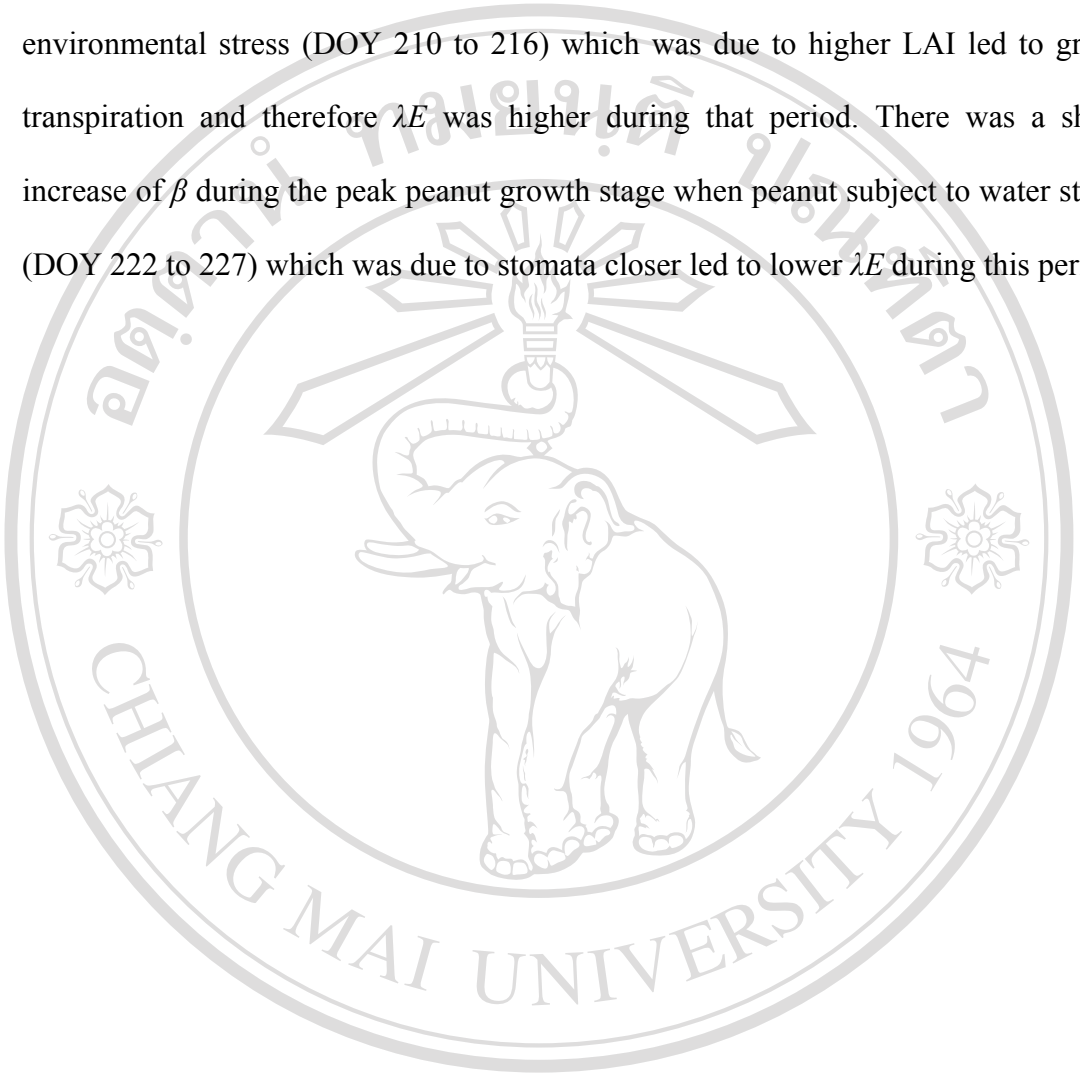

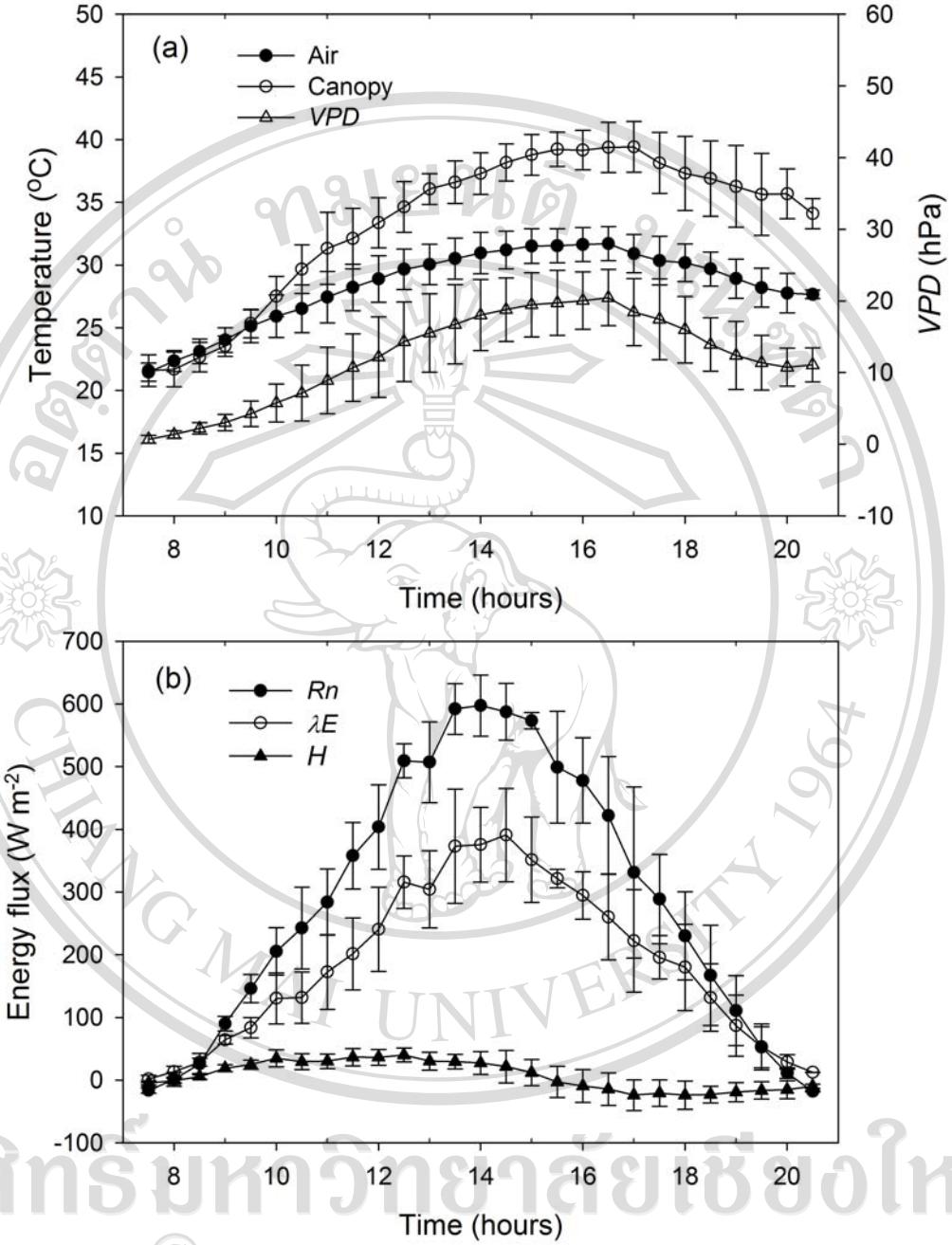




Figure 2.7 Diurnal trends in (a) air temperature, canopy temperature, and vapor pressure deficit (*VPD*) and (b) net radiation (*Rn*), latent heat flux ($\lambda E$) and sensible heat flux (*H*). Data are half-hourly average over the selected 5 days during DOY 210 to 216. Vertical bars indicate standard deviations.

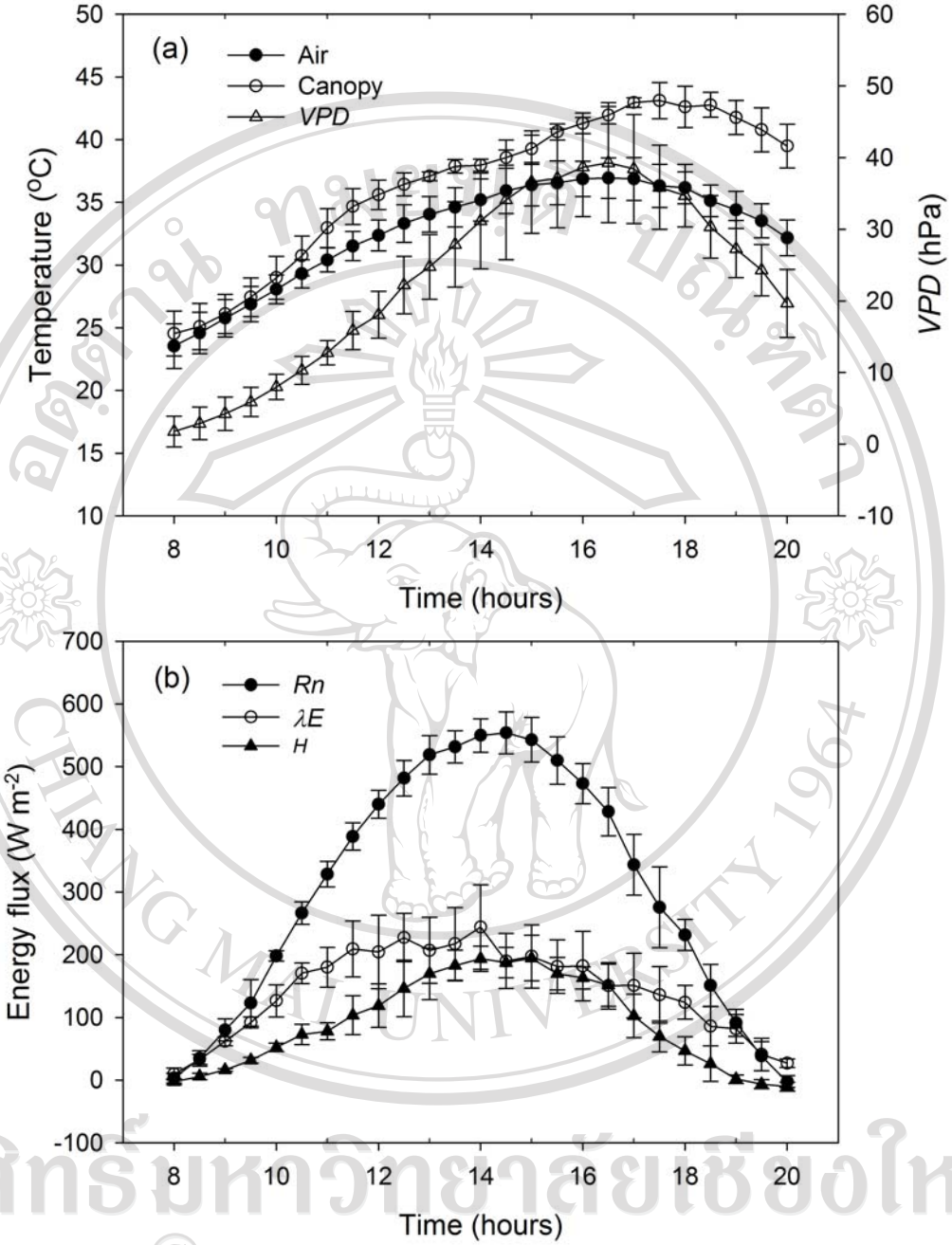




Figure 2.8 Diurnal trends in (a) air temperature, canopy temperature, and vapor pressure deficit (*VPD*) and (b) net radiation (*Rn*), latent heat flux (*λE*) and sensible heat flux (*H*). Data are half-hourly average over the selected 5 days during DOY 222 to 227. Vertical bars indicate standard deviations.

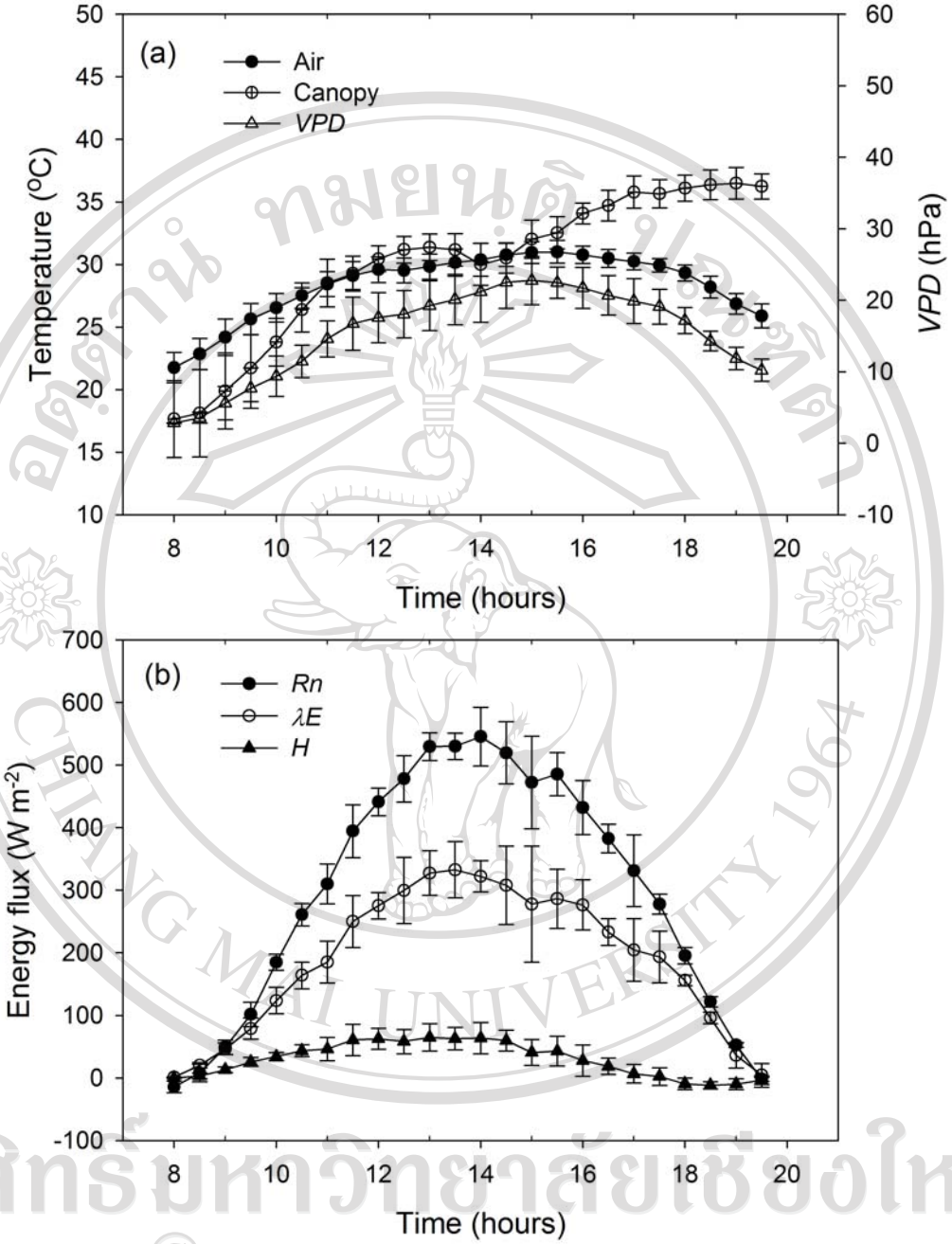




Figure 2.9 Diurnal trends in (a) air temperature, canopy temperature, and vapor pressure deficit (*VPD*) and (b) net radiation (*Rn*), latent heat flux ($\lambda E$) and sensible heat flux (*H*). Data are half-hourly average over the selected 5 days during DOY 248 to 254. Vertical bars indicate standard deviations.

**Diurnal patterns of $CO_2$ and $H_2O$ exchange**

Over the course of the growing season, the variations in daytime carbon dioxide and evapotranspiration exchange depend on growth stage of canopy and available soil water during the measurement. The course of daytime *NEE* on the water-stress (DOY 220 to 227 and DOY 248 to 254) and non-stress days (DOY 210 to 216) was similar until about mid-morning (Figure 2.10a, b, and c). After that time, a significant divergence in the values of daytime *NEE* occurred. During the reproductive growth period with non-stress (DOY 210 to 216), daytime *NEE* followed similar to the pattern for solar radiation (*Rg*), reached the highest values at the maximum *Rg* (Figure 2.10a). The relationship between daytime *NEE* and *Rg* can be explained by rectangular hyperbola equation (light response) (Figure 2.11a). Daytime *NEE* data obtained during the morning become curvilinear compared to those collected during the afternoon. However, daytime *NEE* values measured in the afternoon were comparable to those detected in the morning ($P>0.05$) (Figure 2.11a). The evapotranspiration (*E*) increased linearly with increasing solar radiation (Figure 2.13 a) and reaching the highest value at around 14:30 h (Figure 2.12a). *E* did not show difference between morning and afternoon ($P>0.05$) (Figure 2.13 a). Ecosystem water use efficiency (*EWUE*), calculated as a ratio between daytime *NEE* and *E*, showed the highest values in the morning as compared to afternoon (Figure 2.12a). A daily peak of *EWUE* occurred at 09:30 h and then decreased, reaching 4.3 $\mu molCO_2$ $mmolH_2O^{-1}$ at the end of the morning and maintained an almost constant value of about 3.0 $\mu molCO_2$ $mmolH_2O^{-1}$ in the afternoon (Figure 2.12a). Between mid-morning and mid-afternoon reductions in *EWUE* were correlated with increases in the atmosphere's *VPD* (Figure 2.7a and Figure 2.12a). Daytime *NEE* and *E* values

measured in the afternoon were comparable to those detected in the morning and the increase of *E* with rising temperature and *VPD* from morning to mid-afternoon indicates that environmental conditions were not limiting for ecosystem gas exchange on this period. High *VPD* is known to induce an increase in transpiration rates leading to reduction in leaf water potential (Hsiao, 1990) and , if water supply is limiting, to a stomatal closure. This was not the case of peanut crop in this period because *VPD* values were low ($0 < VPD < 20$ hPa) (Figure 2.7a) and soil water content was sufficient to compensate for water loss by evapotranspiration.

The responses of daytime *NEE* to water stress at the reproductive growth stage (DOY 220 to 227) and the maturity growth stage (DOY 248 to 254) were difference. During the reproductive growth period (DOY 222 to 227), the relationship between daytime *NEE* and *Rg* did not follow the rectangular hyperbola equation (Figure 2.11b). Daytime *NEE* increased with increasing solar radiation, reaching the maximum value at solar radiation of $512 \pm 18$ W $m^{-2}$ at around mid-morning and then rapidly decreased, approaching below zero in the afternoon (Figure 2.10b). These reductions were attributable to water deficit with high air temperature and high *VPD*. Moreover, daytime *NEE* show a hysteresis in response to solar radiation, which *NEE* measured in the morning were significant higher than those measured in the afternoon ($P<0.001$) (Figure 2.11b). The suppression of daytime *NEE* was due to decreased surface conductance when *VPD* was high. The surface conductance ($g_s$) calculated with Equation 2.2 was usually high in the early morning but declined rapidly as solar radiation and *VPD* increased (Figure 2.14b). In the afternoon the decreasing rate of $g_s$ slowed down and the recovery of $g_s$ was very slight because of the reduced plant transpiration and soil evaporation, which were both limited by the low soil water

content. The midday drop of *E* was less remarkable compare to *NEE* (Figure 2.12b). *E* increased linearly with increasing solar radiation and the *E* values measured in the morning were similar to those measured in the afternoon ($P$>0.05) (Figure 2.13b). This may correspond to leaf wilting allows the light to penetrate in the lower layers of the canopy thus determining high *E* in the afternoon (Vitale *et al.*, 2007).

Both *NEE* and *E* were significantly lower as compared to value measured on DOY 210 to 216 (Figure 2.10a, b and Figure 2.12a, b). *EWUE* showed a similar pattern as detected on DOY 210 to 216, however, the *EWUE* remained constant and reached the values nearly zero throughout the afternoon (Figure 2.12b). The reduction in *EWUE* values is in agreement with experimental data of Vitale *et al.* (2007) in maize and Baldocchi *et al.* (1983) and Rawson *et al.* (1978) in soybean. They found lower water use efficiency in crop plants exposed to water stress as compared to non stressed plants because of stomatal closure. The conservative influence of decreased stomatal conductance in stressed plants was negated by reduced the rate of diffusion $CO_2$ into the leaf and increased the *VPD* between the leaf and the atmosphere caused by associated higher leaf temperature (Craufurad *et al.*, 2000). The present study shows that canopy temperature (Figure 2.7a and 2.8a) and $g_s$ (Figure 2.14a, b) were greater and lower, respectively, on the water stress period. Moreover, the present study also found that the *VPD* was greater when the crop was water stressed (Figure 2.7a and 2.8a).

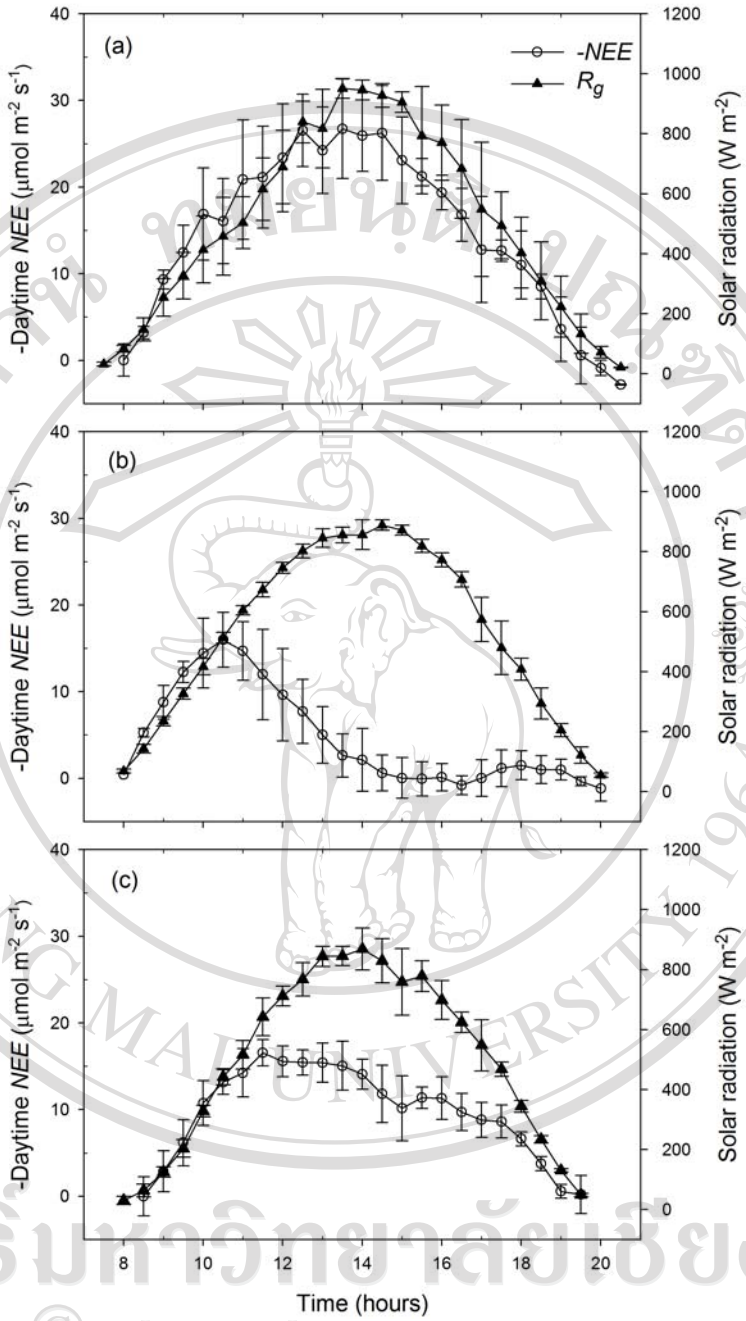




Figure 2.10 Diurnal trends in negative daytime net ecosystem $CO_2$ exchange (*-NEE*) and solar radiation (*Rg*). Data are half-hourly average over the selected 5 days during (a) DOY 210 to 216, (b) DOY 222 to 227, and (c) DOY 248 to 254. Vertical bars indicate standard deviations.

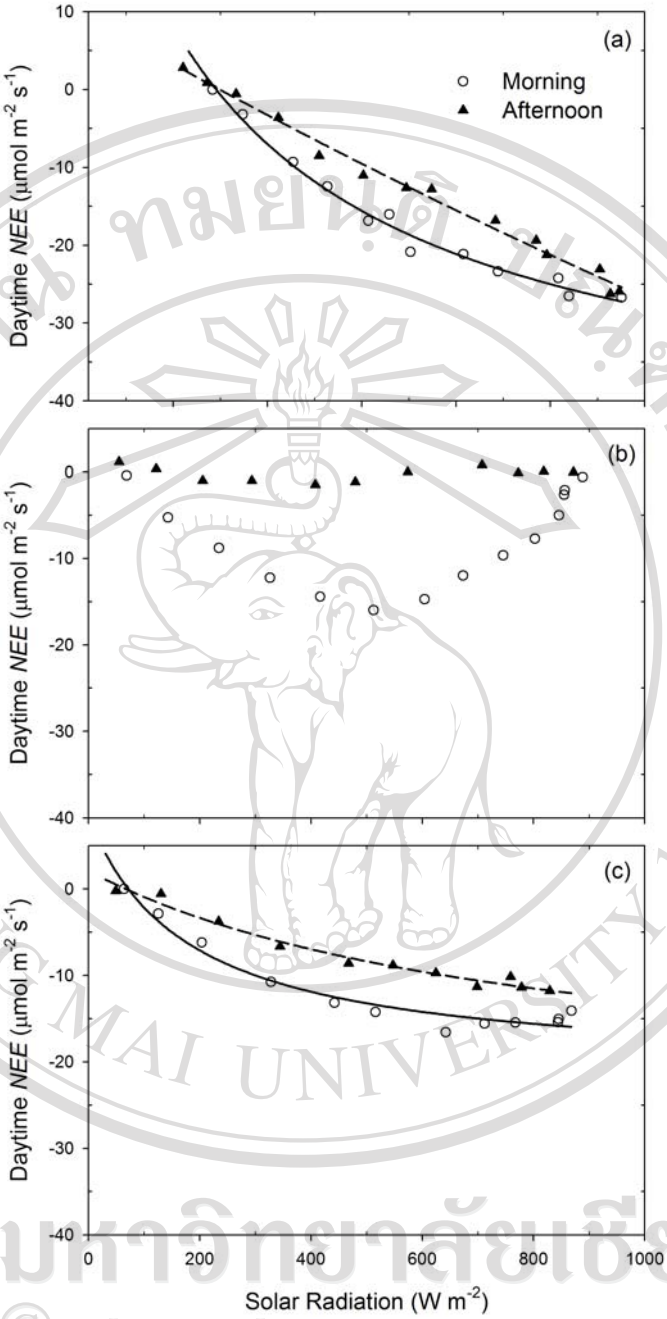




Figure 2.11 The relationship between daytime net ecosystem $CO_2$ exchange (*NEE*) and solar radiation (*Rg*) on the selected 5 days during (a) DOY 210 to 216, (b) DOY 222 to 227, and (c) DOY 248 to 254. A rectangular hyperbola was fitted to explain the relationship between daytime *NEE* and *Rg*.

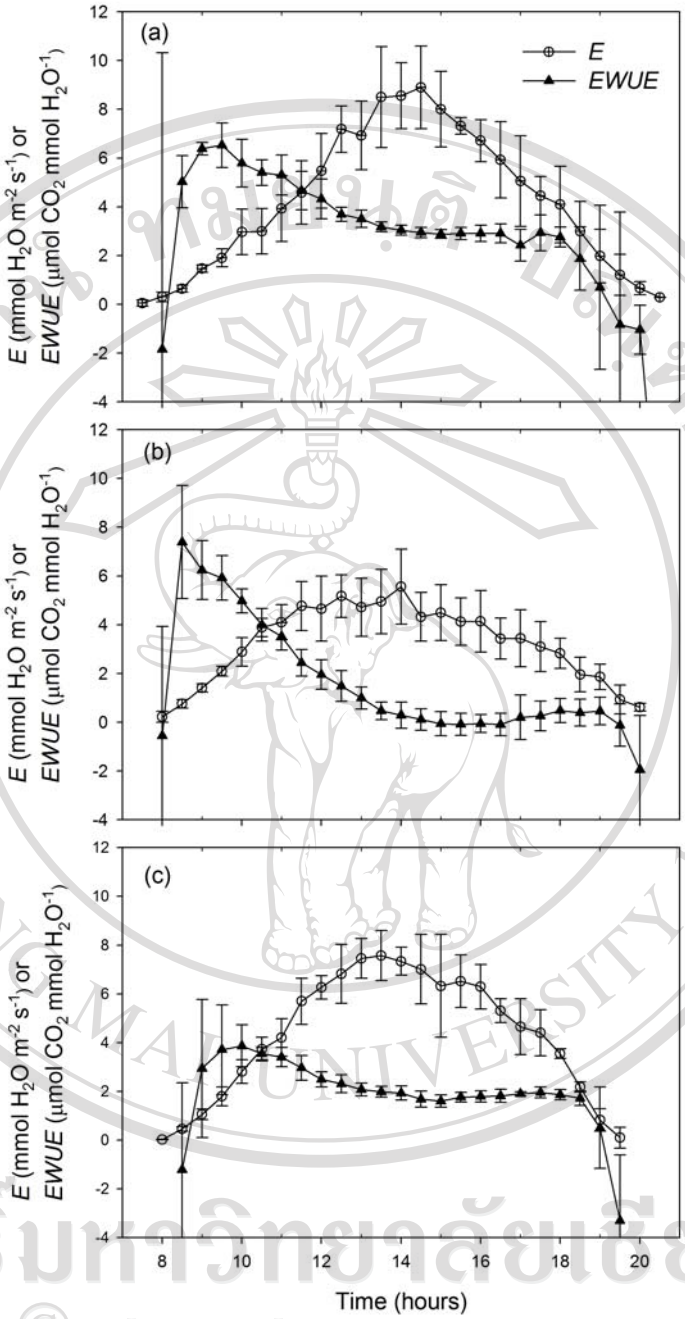


Figure 2.12 Diurnal trends in evapotraspiration (*E*) and ecosystem water use efficiency (*EWUE*). Data are half-hourly average over the selected 5 days during (a) DOY 210 to 216, (b) DOY 222 to 227, and (c) DOY 248 to 254. Vertical bars indicate standard deviations.

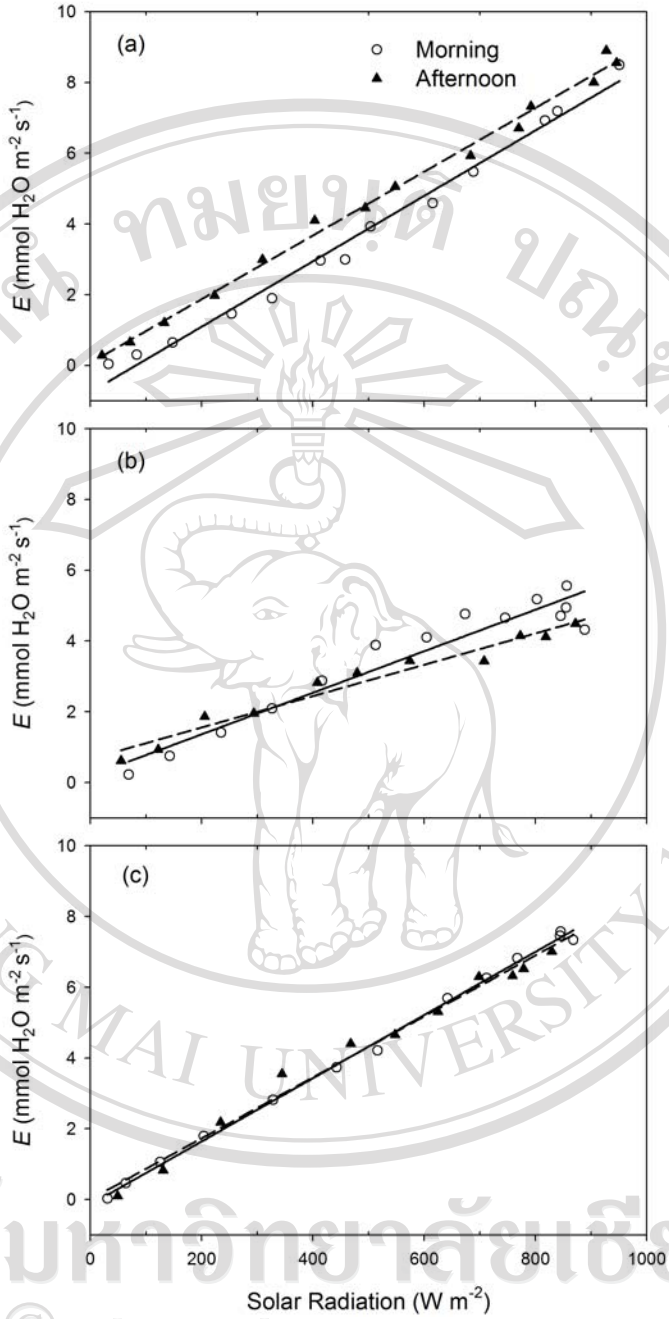




Figure 2.13 The relationship between evapotranspiration (*E*) and solar radiation (*Rg*) on the selected 5 days during (a) DOY 210 to 216, (b) DOY 222 to 227, and (c) DOY 248 to 254. A linear regression was fitted to explain the relationship between *E* and *Rg*.

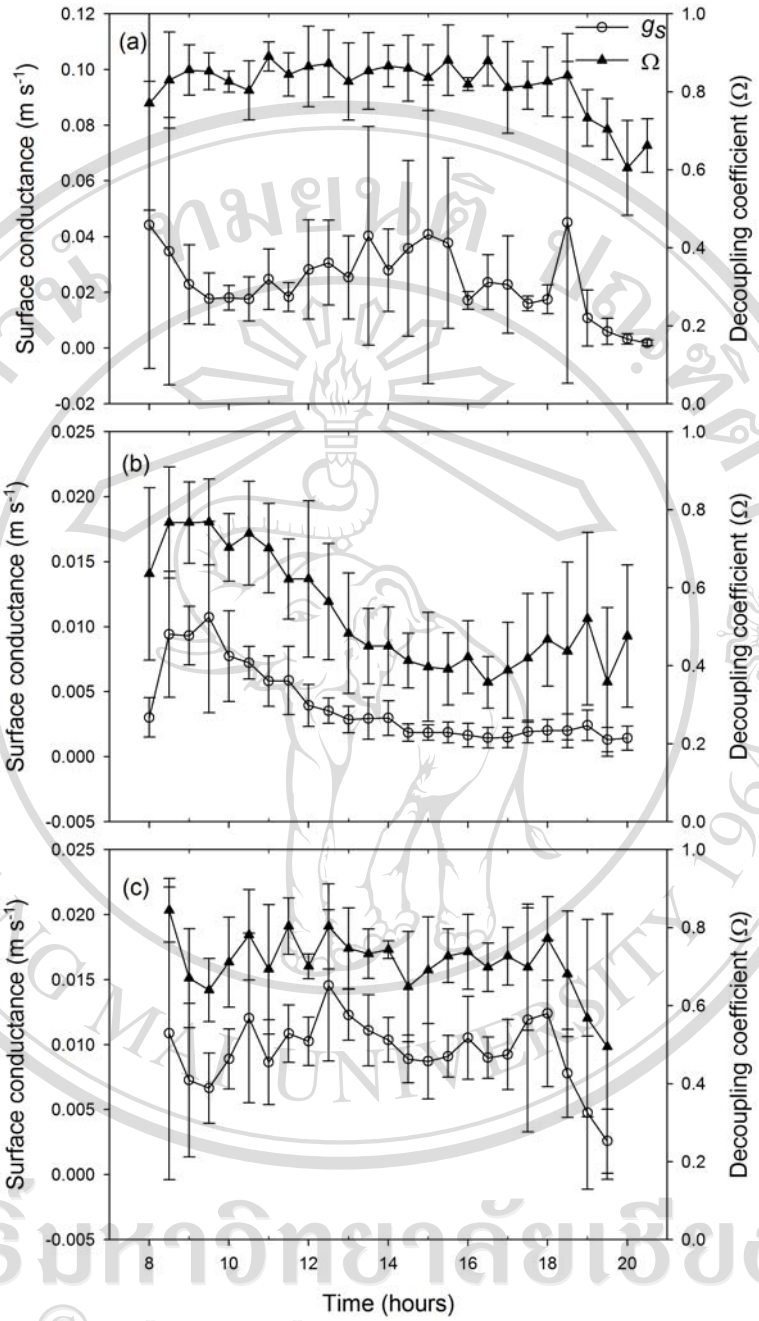




Figure 2.14 (a) Diurnal trends in surface conductance ($g_s$) and decoupling coefficient (Ω). Data are half-hourly average over the selected 5 days during (a) DOY 210 to 216, (b) DOY 222 to 227, and (c) DOY 248 to 254. Vertical bars indicate standard deviations.

The water stress period (DOY 222-227) was also characterized by high air temperature (Figure 2.8a). This factor may has also contributed to the reduction in *EWUE* on this period since high temperature limit plant canopy $CO_2$ exchange and enhance plant and respiration (Baldocchi *et al.*, 1981; Fu *et al.*, 2006). In fact, no difference in evapotranspiration rates between morning and afternoon was observed (Figure 2.13b) but a lower *EWUE* values in the afternoon as compared to morning (Figure 2.12b). Vitale *et al.* (2007) reported that leaf wilting or rolling found in the upper canopy level during the warmest hours of day was responsible for the reduction in *EWUE*.

The depression of *NEE* during DOY 248 to 254 was not significant as that during DOY 222 to 227, in spite of the comparable light intensities at the two periods. The diurnal courses of *Rn* during this period were similar to those during DOY 222 to 227, but air temperature and *VPD* at the period of DOY 248 to 254 (Figure 2.9a) were lower than those detected during DOY 222 to 227 (Figure 2.8a). *NEE* during this period (Figure 2.10c) was a little depressed at midday (11:30 to 14:30 h) and recovered slightly in the afternoon. The little depressed of *NEE* at midday (11:30 to 14:30 h) can be explained by $g_s$ since decreased *NEE* (Figure 2.10c) linearly with decreasing $g_s$ (Figure 2.14c) and the recovered $g_s$ at 15:30 h caused the recovery of *NEE*. The relationship between daytime *NEE* and *Rg* (Figure 2.11c) become strongly curvilinear compared with non-stress days (DOY 210 to 216) (Figure 2.11a). In the morning, daytime *NEE* were comparable to data obtained in the afternoon ($P$>0.05). Moreover, daytime *NEE* reached the saturation at lower *Rg* (about 600 W $m^{-2}$) with those detected on DOY 210 to 216. It may be point out that the curvilinear relationship between daytime *NEE* and *Rg* and low of light saturation point observed

on this period could related to maturity growth stage. The diurnal courses of *E* were similar to those found on DOY 222 to 227, however, the reading values were higher than those period (Figure 2.12c). No difference was observed in *E* values between morning and afternoon ($P>0.05$) (Figure 2.13c). A daily peak of *EWUE* occurred at 10:00 h and then decreased, reaching 2.0 (μmol $CO_2$ mmol $H_2O^{-1}$) at 13:00 h and maintained an almost constant at the same value of 2.0 (μmol $CO_2$ mmol $H_2O^{-1}$) in the afternoon (Figure 2.12c).

To quantify the relative importance of *VPD* in controlling the evapotranspiration on a daily basis, the decoupling coefficient (Ω) (Jarvis and Mcnaughton, 1986) was determined. This coefficient varies from 0 to 1; when it approaches 0, the ecosystem surface and the atmosphere are aerodynamically coupled and the evapotranspiration proceeds at rates imposed by *VPD* and $g_s$; when it approaches 1 the ecosystem surface and the atmosphere are aerodynamically decoupled and the evapotranspiration is controlled by the available energy. Over all, the diurnal pattern of Ω was similar to the changes in $g_s$ (Figure 2.14). Midday (12:00 to 16:00 h) mean Ω values during DOY 210 to 216 and DOY 248 to 254 were generally larger than 0.6, imply that the peanut was decoupled from the atmosphere and the evapotranspiration was mainly depend on the available energy in these period. This result is comparable to the values (about 0.7 to 0.8) reported by Jarvis and McNaughton (1986) for grasslands and crops. During the reproductive growth period with non-stress (DOY 210 to 216) Ω remained fairly constant through the day (Figure 2.14a), indicating that water was available in the soil. Although soil water content at the soil surface reached the lowest values of the whole study period was detected on the maturity growth period (DOY 248 to 254), Ω was also found fairly constant

through the day (Figure 2.14c). This might be because the peanut roots effectively exacted soil water in the deeper soil layer (Allen *et al.*, 1976). In contrast, during the reproductive growth period with water stress (DOY 222 to 227), Ω peaked in the morning and then decreased as the day progressed (Figure 2.14b) and reached the daytime minimal value of about 0.36 in the late afternoon, revealing an increasing control of *VPD* and $g_s$ on *E*. This suggests that, under soil water deficits, the plants reduced the stomatal conductance during the afternoon in response to high temperature and *VPD*, preventing excessive losses of water, as commonly reported (e.g. Aires *et al.*, 2008a; Loustau *et al.*, 1996; Verhoef *et al.*, 1996).